Ocimum sanctum Leaves Prevent Neuronal Cell Apoptosis Through Reduction of Caspase-3 and -9 Expressions and Inhibition of β-amyloid Oligomerization

Dinda Aliffia[1,#], Dinda Ayu Ramadhani[1,#], Widya Wasityastuti[2], Dewi Ratih Tirto Sari[3], Ulayatul Kustiati[1,4], Hevi Wihadmadyatami[1], Dwi Liliek Kusindarta[1,*]

[1]Department of Anatomy, Faculty of Veterinary Medicine, Universitas Gadjah Mada, Jl. Fauna 2, Yogyakarta 55281, Indonesia
[2]Department of Physiology, Faculty of Medicine, Public Health, and Nursing, Universitas Gadjah Mada, Jl. Farmako Sekip Utara, Yogyakarta 55281, Indonesia
[3]Department of Pharmacy, Faculty of Medical Science, Universitas Ibrahimy, Jl. KHR Syamsul Arifin, Situbondo 68375, Indonesia
[4]Veterinary Pharmacology Laboratory, Faculty of Veterinary Medicine, Universitas Brawijaya, Jl. Puncak Dieng, Malang 65151, Indonesia

[#]Both author contribute equally.
*Corresponding author. Email: indarta@ugm.ac.id

Abstract

BACKGROUND: Neurodegenerative diseases are characterized by the loss of neuronal function in the nervous system. In recent years, more than 45 million people worldwide have suffered from progressive loss of memory and cognitive functions caused by Alzheimer's disease. *Ocimum sanctum* is one of the medicinal plants known to have neuroprotective abilities. This study was conducted to elucidate the anti-apoptotic effects of ethanolic extract of *O. sanctum* (EEOS) on PC12 and SH-SY5Y cells as well as interaction between main compounds of EEOS and β-amyloid (Aβ) peptide through *in silico* molecular docking.

METHODS: The viability of TMT-induced PC12 and SH-SY5Y cells was assessed with 3-(4,5-dimethylthiazol-2-yl)-2,5-diphenyl tetrazolium bromide (MTT) assay and acridine orange/propidium iodide staining. Cell proliferation rate was measured with cell counting kit-8 (CCK-8) assay. Nuclear fragmentation was observed with Hoechst 33342 staining. Caspase -3 and -9 expressions were measured using enzyme-linked immunosorbent assay. Interactions between main compounds of EEOS and Aβ were visualized with *in silico* molecular docking.

RESULTS: EEOS had the potential effect of maintaining cell viability, preventing the cell's morphological changes, and inhibiting apoptosis via the caspase pathway in PC12 and SH-SY5Y cells. Meanwhile, flavonoid K, phenol, eugenol could interact with the active site of Aβ through hydrogen-bonding and hydrophobic interactions.

CONCLUSION: EEOS could prevent neuronal cell apoptosis via downregulation of caspase-3 and -9. Main compounds of EEOS could interact with the active site of Aβ, and thereby might inhibit Aβ oligomerization. Thus, EEOS and its main compounds could be potential as neuroprotective agents for preventing neurodegenerative diseases.

KEYWORDS: *Ocimum sanctum*, anti-apoptotic, β-amyloid, caspase, neurodegeneration

Indones Biomed J. 2023; 15(4): 322-32

Introduction

The neuron is the fundamental unit that makes up a nerve pathway. Neurons, as miniature information processors, receive incoming information, send signals to other neurons, and continue to send the signal response to the muscles and glands.(1) Neuronal cell death in normal physiology is limited to the elderly. In pathological conditions, neuronal shrinkage and cell death in certain

brain regions are the basic features of neurodegenerative diseases.(2)

Neurodegeneration leads to irreversible neuronal damage and increased neuronal loss due to metabolic or toxic disorder. Neurodegenerative diseases are caused by mitochondrial dysfunction, glutamate toxicity, calcium load, proteolytic stress, oxidative stress, neuroinflammation, and aging, and protein aggregation.(3) One of the protein aggregates involved in neurogenerative disease is β-amyloid (Aβ). Accumulation of Aβ peptide in the hippocampal and entorhinal cortex promotes Alzheimer's disease (AD). AD is the most common neurodegenerative disease with dementia as a primary clinical sign.(4,5) AD causes an imbalance among the elderly by causing memory loss and personality and behavioral changes such as depression, apathy, social withdrawal, mood swings, irritability, and aggressiveness.(6)

Currently, the treatment of neurodegenerative diseases has not satisfied the patient's conditions. Conventional treatments, such as cholinesterase inhibitors, can reduce the symptoms of AD. However, these treatments have been known to cause several side effects, such as constipation, dizziness, high blood pressure, vomiting, and nausea.(7) Numerous studies to investigate antibody-based treatment with the Aβ peptide as a target, such as ponezumab (8), solanezumab (9), gantenerumab (10), crenezumab (11) have already been done. However, most of the drugs fail on the clinical trial (phase I, II, or III), and force the medication for drawback due to the loss of efficacy and toxicity effects.

Recently, many studies have explored the phytochemical benefits of medicinal plants, which are believed to have promising therapeutic effects with minimal side effects. *Ocimum sanctum* is a medicinal plant widely found in Indonesia and almost all Southeast Asian regions. *O. sanctum* is widely used in Asia due to its anti-inflammatory and anti-oxidative effects.(12) Previous studies have shown that *in vitro* and *in vivo* administration of ethanolic extract of *O. sanctum* (EEOS) on the neurodegeneration model could promote neuron proliferation in the hippocampal cornu ammonis 1 and 3 and maintain the stability of the expression of several neurotransmitters, such as neuropeptide Y, serotonin, acetylcholinesterase (Ach) and choline acetyltransferase (ChAT).(13-15) Therefore, this study was aimed to elucidate the anti-apoptotic effects of EEOS on PC12 and SH-SY5Y cell lines as well as interaction between main active compounds of EEOS and Aβ peptide through *in silico* molecular docking.

Methods

EEOS Preparation

O. sanctum leaf simplicia was obtained from CV Merapi Herbal, Yogyakarta, Indonesia. The simplicia was extracted using the maceration technique. Four L of 96% ethanol (Merck, Darmstadt, Germany) was added to 300 g of *O. sanctum* leaf simplicia. The filtrate was concentrated using a vacuum rotary evaporator (Heidolph, Schwabach, Germany). The weight of the resulting EEOS pasta was 36.6 g.

PC12 and SH-SY5Y Cell Culture

The PC12 cells line were purchased from the American Type Culture Collection (ATCC, Manassas, VA, USA), while the SH-SY5Y cells were purchased from the European Collection of Authentication Cell Cultures (ECACC, Salisbury, UK). The cells were cultured in Dulbecco's modified Eagle medium (DMEM) (Gibco, Auckland, New Zealand) combined with 5% Horse Serum and 10% Fetal Bovine Serum (Capricorn, Ebsdorfergrund, Germany) for PC12 cells, or 5% Fetal Calf Serum for SH-SY5Y cells (Gibco, Auckland, New Zealand), 1% Penicillin-Streptomycin (Capricorn, Ebsdorfergrund, Germany), and 0.5% Amphotericin B (Gibco, Langenselbold, Germany). Unless otherwise noted, all cells were incubated in an incubator at 37°C with 5% CO_2. The cells were then subcultured upon reaching 80% confluence.

Cell Viability Assay

PC12 ($1×10^4$ cells) and SH-SY5Y cells ($2×10^4$ cells) were seeded in a 96-well plate. The cells were treated with/without 10 μM trimethyltin (TMT) (Sigma-Aldrich, Langenselbold, Germany) and 1 μM Donepezil HCl (Sigma, Langenselbold, Germany) or 50, 75, or 100 μg/mL EEOS for 24 hours. The media was then aspirated, and each well was rinsed with Dulbecco's phosphate-buffered saline (DPBS). After that, 0.5 mg/mL of 3-(4,5-dimethylthiazol-2-yl)-2,5-diphenyl tetrazolium bromide (MTT) reagent (Roche, Mannheim, Germany) was added to each well. The samples were incubated for four hours. The MTT reagent was aspirated, and 100 μL of DMSO were added to each well. The absorbance of the plate was read at a wavelength of 595 nm.

Proliferation Assay

PC12 ($1×10^4$ cells) and SH-SY5Y cells ($2×10^4$ cells) were seeded in a 96-well plate. After 24 hours, the cells were

treated with/without 10 µM TMT and 1 µM Donepezil HCl or 50, 75, or 100 µg/mL EEOS for another 24 hours. Cell counting kit-8 (CCK-8) reagent (Abbkine, Wuhan, China) and DMEM were then added to each well. The absorbance of the plate was read at a wavelength of 450 nm.

Acridine Orange/Propidium Iodide (AO/PI) Staining

PC12 ($5×10^4$ cells) and SH-SY5Y cells ($5×10^4$ cells) were cultivated in 24-well plates, which had been covered with poly-lysine coated coverslip and incubated for 24 hours. After the cells reached 50% confluency, the cells were treated with/without 10 µM TMT and 1 µM Donepezil HCl or 50, 75, or 100 µg/mL EEOS for 24 hours. After incubation, the cells were washed with DPBS. The cells were stained with 50 µg/mL AO and 50 µg/mL PI and observed under a confocal microscope (Leica, Wetzlar, Germany).

Hoechst 33342 Staining

PC12 ($5×10^4$ cells) and SH-SY5Y cells ($5×10^4$ cells) were cultivated in 24-well plates covered with a coverslip and incubated for 24 h. After the cells reached 50% confluency, the cells were treated with/without 10 µM TMT and 1 µM Donepezil HCl or 50, 75, or 100 µg/mL EEOS for 24 hours. The cells were then rinsed with DPBS and fixed with ice-cold 70% ethanol for 15 minutes. The fixative was removed, and 1 µg/mL of Hoechst 33342 staining solution was added to each well under dark room conditions and incubated for 10 minutes. The cells were washed with DPBS for 5 minutes. The cells were observed under a confocal microscope (Leica, Wetzlar, Germany).

PC12 and SH-SY5Y Cell Lysates Preparation

PC12 cells ($5×10^5$ cells) and SH-SY5Y cells ($5×10^4$ cells), which were cultured in a 6-well plate, were washed with DPBS. The cells were treated with/without 10 µM TMT and 1 µM Donepezil HCl or 50, 75, or 100 µg/mL EEOS for 24 hours. Radioimmunoprecipitation (RIPA) lysis buffer (Santa Cruz Biotechnology, Texas, TX, USA) was added to each well. The plate was then gently shaken and allowed to stand for 15 minutes. The cells were harvested and lysed, and the cell lysate was centrifuged at 10,000 rpm for 10 minutes at 4°C. The supernatant was collected for further assay.

Enzyme-linked Immunosorbent Assay (ELISA) for Caspase-3 and -9

The expression levels of caspase-3 and -9 in the cell lysate were measured with caspase-3 and -9 ELISA kits (Fine Test, Wuhan, China) according to the manufacturer's

instruction. The plates were read at a wavelength of 450 nm using an ELISA reader (Tecan Spark 20M, Mannedorf, Switzerland).

Statistical Analysis

The absorbance values obtained from MTT assay, CCK-8 assay and ELISA were analyzed using GraphPad Prism software v. 7 (Proteogenomics Research Institute for Systems Medicine (PRISM), La Jolla, CA, USA) with one-way ANOVA and followed by a Tukey's honestly significant difference (HSD) test.

Ligand and Protein Preparation for *in silico* Analysis

The chemical structures of flavonoid K (CID 5317287), phenol (CID 996) eugenol (CID 3314), and donepezil (CID 3152) were downloaded from the National Center of Biotechnology Information (NCBI) PubChem database (https://pubchem.ncbi.nlm.nih.gov/). The three-dimensional (3D) structure of Aβ peptide was downloaded from the Protein Data Bank (PDB) (https://www.rcsb.org/) database (PDB ID 1AAP). Protein structure optimization was performed to remove the molecules that make up the solvent/solvent and attached ligands. The protein structure was then predicted for its active site using the Molegro Virtual Docker 5 (Informer Technologies, Los Angeles, CA, USA) program with binding cavities parameters as follows: van der Waals, maximum cavities 5.

Docking Simulation

Flavonoid K, phenol, eugenol, and donepezil were docked with Aβ peptide using the Molegro Virtual Docker 5 software on the following coordinates: X = 11.98; Y=18.92; Z=36.62; Radius 15. The docking parameters were as follows: Score Function Moldock Score [Grid]; grid resolution 0.30; algorithm MolDock SE; Number of Runs 10, Max iteration 1500; max population size 50; pose generation energy threshold 100, tries 10-30; simplex evolution max steps 300; neighbor distance factor 1.00; multiple poses several poses 5; energy threshold 0.00; cluster similar poses RMSD threshold 1.

Docking Data Analysis

The molecular docking results were superimposed with PyMol software version 2.2 (Scrhodinger, New York, NY, USA). Discovery Studio program (Dassault Systemes BIOVIA, New York, NY, USA) version 21.1.1 was used to visualize the interactions between the active compounds and the target protein.

Results

EEOS Maintained Viability and Promoted Proliferation of TMT-induced PC12 and SH-SY5Y cells

The viability percentage of TMT + 50 or 100 μg/mL EEOS-treated PC12 and SHSY-5Y cells were significantly higher than those of TMT-induced PC12 and SHSY-5Y cells. These results were similar with the viability percentage of the untreated cells (Figure 1A, Figure 1B). Furthermore, the proliferation rate of TMT + 50, 75, or 100 μg/mL EEOS-treated PC12 and SHSY-5Y cells were significantly higher than those of TMT-induced PC12 and SHSY-5Y cells. These results were similar with the proliferation rate of the untreated and TMT + Donepezil HCl-treated cells. (Figure 1C, Figure 1D). In addition, microscopic observation

with Acridine Orange/Propidium Iodide (AO/PI) staining demonstrated that EEOS increased the number of viable PC12 and SHSY-5Y cells in a concentration-dependent manner. Viability of TMT + EEOS-treated cells was similar with that of untreated and TMT + Donepezil HCl-treated cells (Figure 2).

EEOS Decreased Caspase-3 and -9 Expressions in TMT-induced PC-12 and SH-SY5Y Cells

TMT + EEOS-treated PC-12 and SH-SY5Y cells showed significant lower expressions of caspase-3 (Figure 3A, Figure 3B) and -9 (Figure 3C, Figure 3D) in comparison with TMT-induced cells. TMT + 100 μg/mL EEOS-treated PC12 and SHSY-5Y cells had lower caspase-3 and -9 expressions. These results were similar with the expression levels of caspase-3 and -9 of TMT + Donepezil
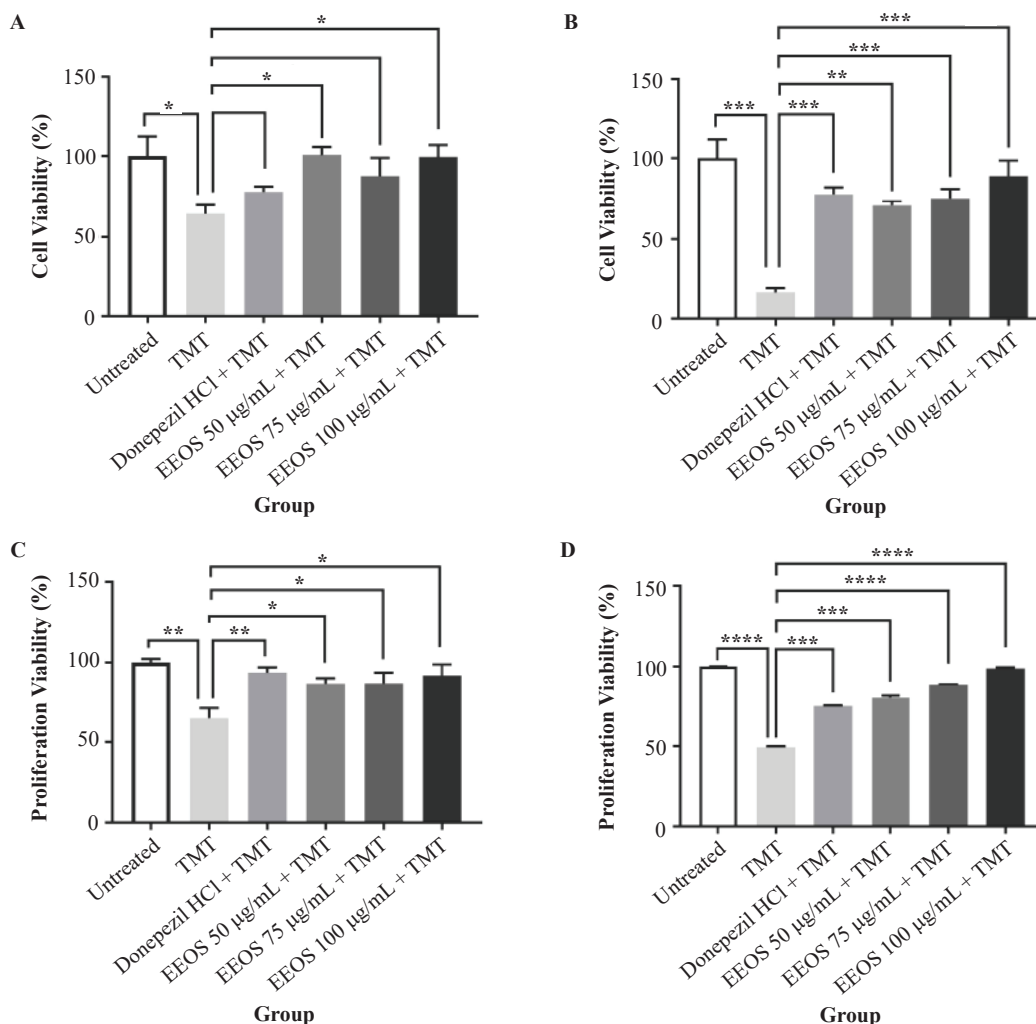

Figure 1. EEOS maintained viability and promoted proliferation of TMT-induced PC-12 and SH-SY5Y cells. Cell viability and proliferation rate were measured with MTT and CCK-8 assays, respectively. A: Cellular viability of PC12 cells; B: Cellular viability of SH-SY5Y cells; C: Cell proliferation rate in PC-12 cells; D: Cell proliferation rate in SH-SY5Y cell line. Tukey's HSD test, *$0.05{\geq}p{>}0.01$; **$0.01{\geq}p{>}0.001$; ***$0.001{\geq}p{>}0.0001$; ****$p{\leq}0.0001$.
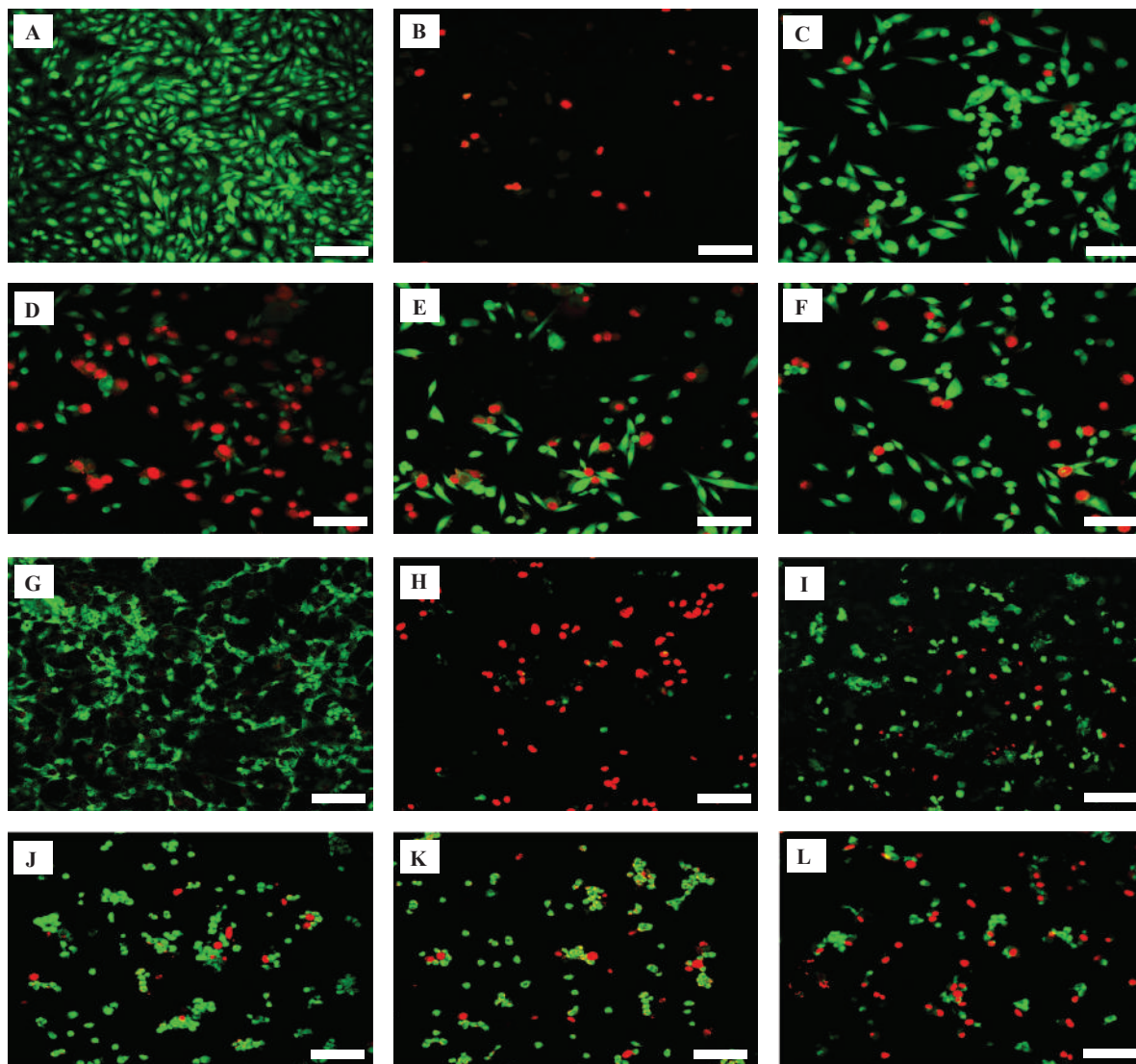
Figure 2. EEOS prevented apoptosis of TMT-induced PC12 and SH-SY5Y cells. The viability of in PC12 and SH-SY5Y cells was assessed with AO/PI staining. Red color: Cells undergoing apoptosis; Green color: Viable cells. Green-colored cells were observed to be dominant in groups treated with higher concentrations of EEOS. A: Untreated PC12; B: PC12 + TMT; C: PC12 + TMT + Donepezil; D: PC12 + TMT + 50 µg/mL EEOS; E: PC12 + TMT + 75 µg/mL EEOS; F: PC12 + TMT + 100 µg/mL EEOS; G: Untreated SH-SY5Y; H: SH-SY5Y + TMT; I: SH-SY5Y + TMT + Donepezil; J: SH-SY5Y + TMT + 50 µg/mL EEOS; K: SH-SY5Y + TMT + 75 µg/mL EEOS; L: SH-SY5Y + TMT + 100 µg/mL EEOS. White bar: 40 µm.

HCl-treated cells. To strengthen the ELISA results, nucleus morphological analysis was performed using Hoechst 33342 stain. EEOS reduced nuclear fragmentation in both PC12 and SH-SY5Y cells in a concentration-dependent manner. Nuclear fragmentation in TMT + EEOS-treated cells was similar with those in the untreated and TMT + Donepezil HCl-treated cells (Figure 4).

EEOS Phytochemical Compounds Interacted with the Active Site of Aβ Peptide

Flavonoid K bound to Aβ peptide with 11 hydrogen bonds, as well as one electrostatic and eight hydrophobic interactions. The binding energy of flavonoid K-Aβ complex was -271.6 kJ/mol. Flavonoid K-bound active-site residues were PHE34, THR26, PRO32, TYR22, ASP24, THR11, ALA9, and PHE33 (Table 1, Figure 5). Phenol bound to Aβ peptide with two hydrogen bonds at residues GLN8 and ASP24 and one hydrophobic bond at residues ALA9. The binding energy for this interaction was -136.5 kJ/mol (Table 1, Figure 5). In addition, eugenol bound to Aβ peptide through two hydrogen bonds at the THR26 and ASP24 residues, one electrostatic interaction at the ASP24 residue, and three hydrophobic interactions at the ALA9, VAL25, and ALA9 residues. The energy formed is -198.75 kJ/mol, which was lower than the one of phenol (Table 1, Figure 5). Donepezil interacted with VAL18, ALA21, and VAL24 residues of Aβ-
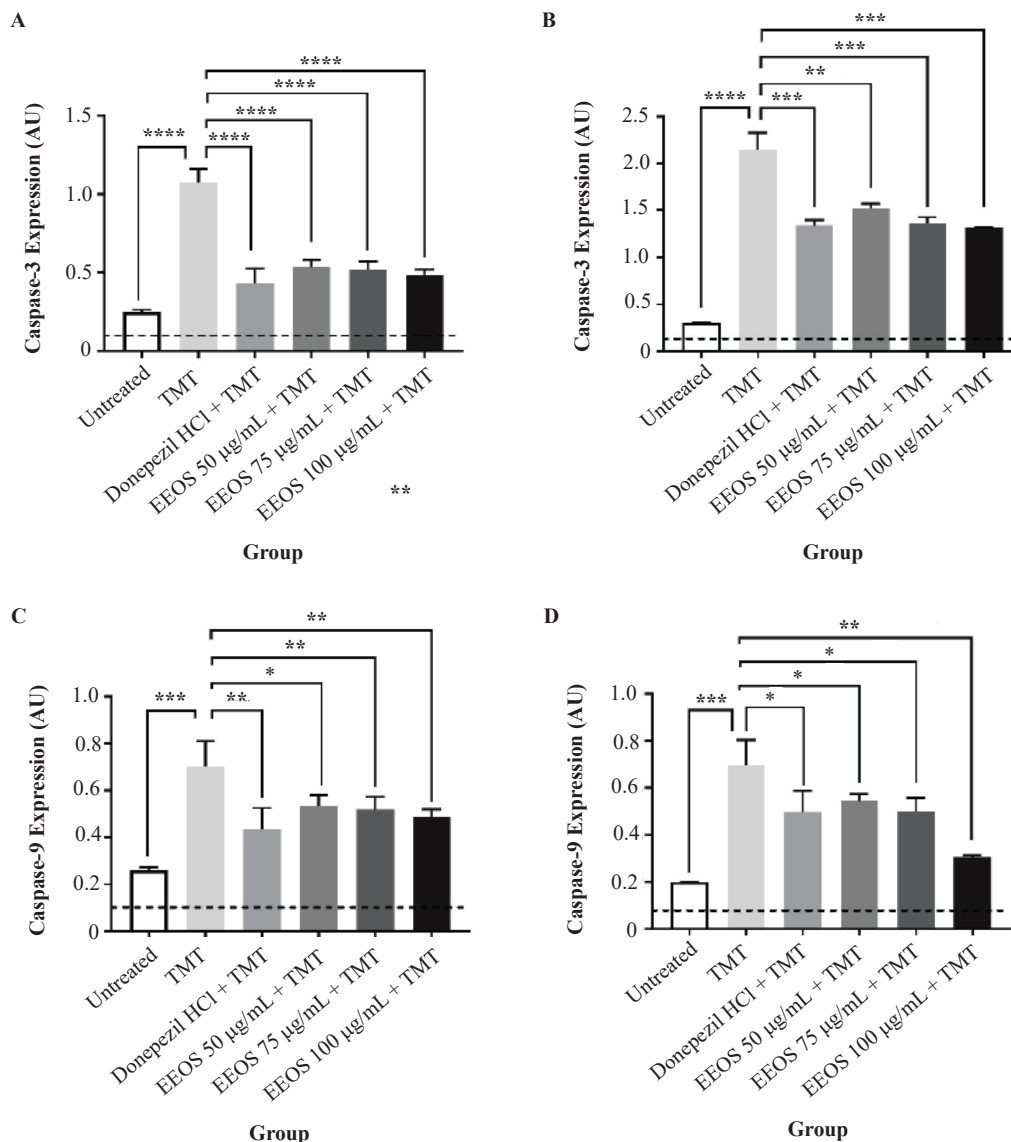
A

B

C

D

Figure 3. EEOS decreased caspase-3 and -9 expressions in TMT-induced PC-12 and SH-SY5Y cell lines. Cell lysates of PC-12 and SH-SY5Y cells were subjected to ELISA to measure caspase-3 and -9 expressions. A: Expression of caspase-3 in PC12 cells; B: Expression of caspase-3 in SH-SY5Y cells; C: Expression of caspase-9 in PC-12 cells; D: Expression of caspase-9 in SH-SY5Y cells. Tukey's HSD test, *$0.05 \geq p > 0.01$; **$0.01 \geq p > 0.001$; ***$0.001 \geq p > 0.0001$; ****$p \leq 0.0001$.

peptide through hydrophobic interaction (Table 1, Figure 5). Besides, several amino acid residues interacted through van der Waals interaction were identified, including GLU22, GLY25, LYS28, MET35, ILE31, and LEU34 (Figure 5).

Discussion

Herbal medicine has long been trusted as an alternative therapy for treating various diseases (16,17) and has been known to increase proliferation of several types of cells (18). In this research, the potency of EEOS to protect the neuron from apoptosis in neurodegenerative diseases was

investigated. Phytochemical substances are suggested to play a pivotal role in the antiapoptotic activities of medicinal plants.(19)

In this study, EEOS maintained the viability of the TMT-induced PC12 and SH-SY5Y cells. This result is in line with the previous studies showed that EEOS maintained the stability of several neurotransmitter, such as ChAT in human cerebral microvascular endothelial cells and HEK-293 cells as *in vitro* model neurodegeneration induced by TMT.(13,14,20,21)

In addition, EEOS reduced nuclear fragmentation in a concentration-dependent manner (22,23) and decreased the expression levels of caspase-3 and -9. Neuroinflammation
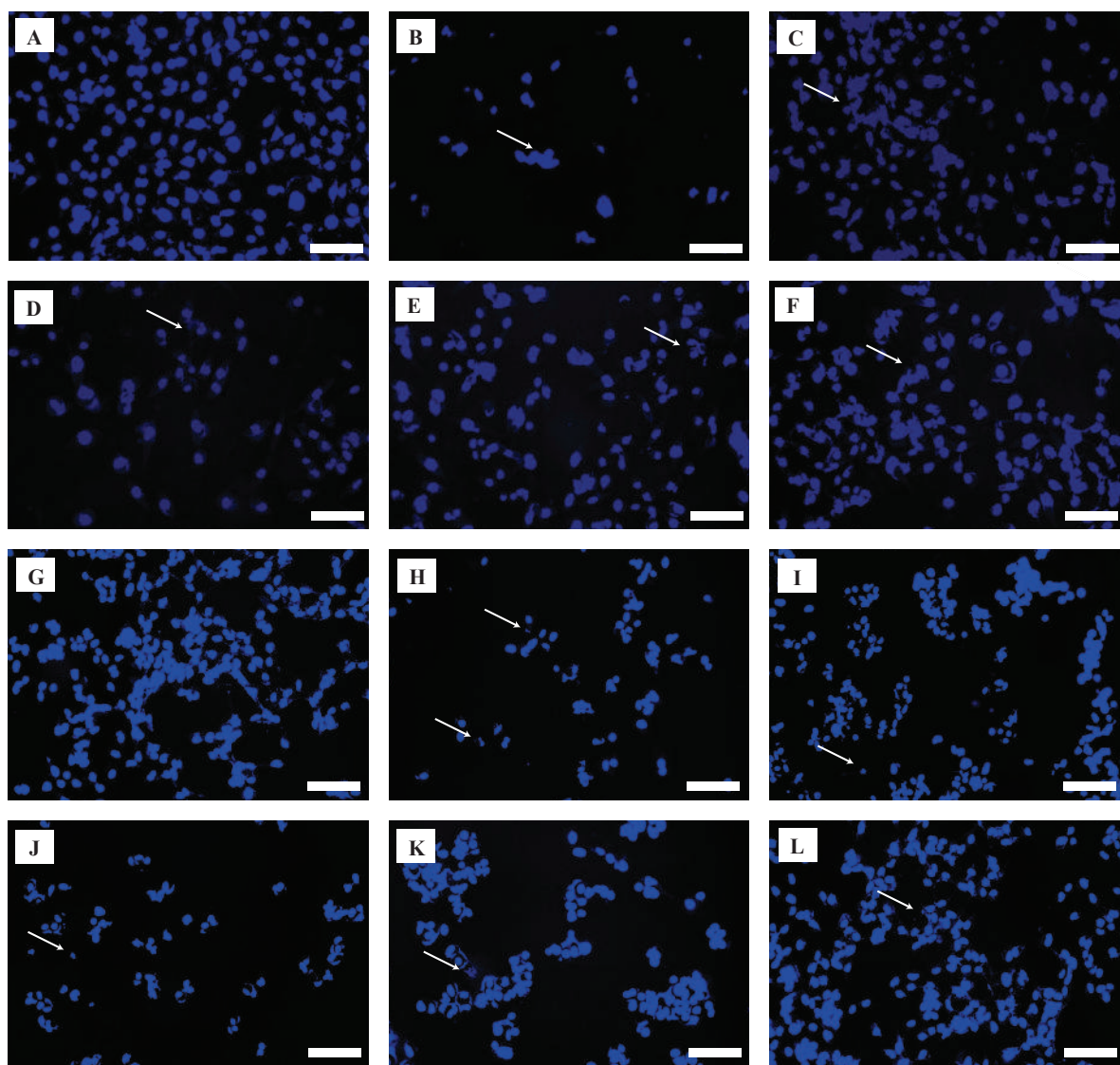
Figure 4. EEOS inhibited nuclear fragmentation in PC12 and SH-SY5Y cells. Nuclear fragmentation in PC12 and SH-SY5Y cells was assessed with Hoechst 33342 staining. Arrows: Nuclear fragmentation. Less nuclear fragmentation was observed in cells treated with higher concentrations of EEOS. A: Untreated PC12; B: PC12 + TMT; C: PC12 + TMT + Donepezil; D: PC12 + TMT + 50 µg/mL EEOS; E: PC12 + TMT + 75 µg/mL EEOS; F: PC12 + TMT + 100 µg/mL EEOS; G: Untreated SH-SY5Y; H: SH-SY5Y + TMT; I: SH-SY5Y + TMT + Donepezil; J: SH-SY5Y + TMT + 50 µg/mL EEOS; K: SH-SY5Y + TMT + 75 µg/mL EEOS; L: SH-SY5Y + TMT + 100 µg/mL EEOS. White bar: 40 µm.

and neuronal loss have a crucial role in the development of AD.(24) Apoptosis is a cellular process that regulates cell death under physiological or pathological stimuli. Alzheimer's (AD) is a chronic neurodegenerative disease with dysregulated apoptotic cascade and abnormal neuronal loss. Activation of caspases, which play an important role in apoptosis, is associated with increased Aβ production, co-localizes with neurofibrillary tangles, and degenerative granulovacuolar changes in the hippocampus.(25)

It has been reported that EEOS contained flavonoid K, eugenol, and phenol.(26) In the present study, flavonoid K showed a higher hydrophobicity than phenol and eugenol.

Meanwhile, the hydrogen bond profile showed the presence of hydrogen donors and acceptors in flavonoid K, and hydrogen acceptors in phenol and eugenol. The binding energy of flavonoid K was lower than those of eugenol and phenol. The lower the binding energy of a compound, the stronger the interaction.(27) Moreover, these three compounds interacted at the Aβ active site, indicating that they had potency as therapeutic agents for neurological diseases (AD). Aβ is a crucial target in AD treatment (28), since Aβ plaques deposit in the central nervous system can cause the deficit of spatial learning and memory in AD (4). Prolonged exposures of Aβ can stimulate excitotoxicity and

Table 1. Binding energy, interaction, and chemical bond between flavonoid K, phenol, eugenol, and Donepezil and Aβ.

Ligand	Binding Energy (kJ/mol)	Interactions	Distance (Å)	Category	Types
Flavonoid K	-271.60	A:PHE34:N - :10:O2	3.03548	Hydrogen Bond	Conventional Hydrogen Bond
		A:PHE34:N - :10:O3	3.27306	Hydrogen Bond	Conventional Hydrogen Bond
		B:THR26:OG1 - :10:O1	3.00244	Hydrogen Bond	Conventional Hydrogen Bond
		:10:H5 - A:PRO32:O	2.22375	Hydrogen Bond	Conventional Hydrogen Bond
		:10:H6 - A:TYR22:OH	1.62537	Hydrogen Bond	Conventional Hydrogen Bond
		:10:H13 - B:TYR22:OH	2.61064	Hydrogen Bond	Conventional Hydrogen Bond
		:10:H13 - B:ASP24:OD1	1.61598	Hydrogen Bond	Conventional Hydrogen Bond
		:10:H9 - :10:O4	2.28386	Hydrogen Bond	Carbon Hydrogen Bond
		:10:H11 - A:THR11:OG1	2.52597	Hydrogen Bond	Carbon Hydrogen Bond
		:10:H15 - :10:O8	2.36482	Hydrogen Bond	Carbon Hydrogen Bond
		A:ASP24:OD1 - :10	4.63129	Electrostatic	Pi-Anion
		A:TYR22:OH - :10	3.98424	Hydrogen Bond	Pi-Donor Hydrogen Bond
		A:TYR22 - :10	5.1937	Hydrophobic	Pi-Pi Stacked
		A:PHE33 - :10	5.82446	Hydrophobic	Pi-Pi T-shaped
		B:ALA9 - :10:C18	4.4155	Hydrophobic	Alkyl
		A:PHE34 - :10:C16	4.44711	Hydrophobic	Pi-Alkyl
		B:TYR22 - :10:C18	5.09443	Hydrophobic	Pi-Alkyl
		:10 - A:ALA9	4.29292	Hydrophobic	Pi-Alkyl
		:10 - A:ALA9	481,357	Hydrophobic	Pi-Alkyl
		:10 - A:ALA9	4.81581	Hydrophobic	Pi-Alkyl
Phenol	-136.50	:10:H6 - A:GLN8:OE1	2.20711	Hydrogen Bond	Conventional Hydrogen Bond
		:10:H6 - B:ASP24:OD2	2.74898	Hydrogen Bond	Conventional Hydrogen Bond
		:10 - A:ALA9	4.79577	Hydrophobic	Pi-Alkyl
Eugenol	-198.75	:10:H10 - B:THR26:OG1	2.26762	Hydrogen Bond	Conventional Hydrogen Bond
		:10:H7 - B:ASP24:OD1	2.76509	Hydrogen Bond	Carbon Hydrogen Bond
		A:ASP24:OD1 - :10	4.89078	Electrostatic	Pi-Anion
		B:ALA9 - :10:C10	4.27365	Hydrophobic	Alkyl
		:10:C10 - A:VAL25	5.39072	Hydrophobic	Alkyl
		:10 - A:ALA9	4.72929	Hydrophobic	Pi-Alkyl
Donepizil	-394.80	:10:C23 - A:VAL18	500,255	Hydrophobic	Alkyl
		:10:C24 - A:VAL18	39,502	Hydrophobic	Alkyl
		:10 - A:ALA21	448,029	Hydrophobic	Pi-Alkyl
		:10 - A:VAL24	518,883	Hydrophobic	Pi-Alkyl
		:10:H8 - :10:H13	13,077	Unfavorable	Unfavorable Bump

causing neuronal death. Cell cycle re-entry can provoke neuronal apoptosis in AD patient with Aβ deposit.(29) Aβ can promote the activation of inflammatory microglia to suppress and prevent phagocytic activity from clearing Aβ plaques and induce progressive neuronal degeneration. (24,30)

One of the focuses of AD treatment is to prevent neuronal cell death. Flavonoid K, which is also called as phytoestrogen, has a basic chemical structure similar to estrogen. In neurodegenerative diseases, flavonoid K could reduce cellular stress, and have antioxidant, anti-inflammatory, and anti-apoptotic properties. Flavonoid K have been shown to interact with various signaling proteins, modulating several signaling pathways, and functioning as a neuroprotective compound.(31,32) As antioxidant, phenol has been proven to have anti-

inflammatory properties. Preclinical studies demonstrated that phenol could exert its neuroprotective effects by targeting multiple cellular pathways, including protection from neuronal inflammation, oxidative damage, autophagy, and apoptosis.(33,34)

Conclusion

EEOS could prevent neuronal cell apoptosis via reduction of caspase-3 and -9 expressions. Main compounds of EEOS, namely flavonoid K, phenol, and eugenol, could interact with the active site of Aβ, and thereby might inhibit Aβ oligomerization. Thus, EEOS and its main compounds could be potential as neuroprotective agents for preventing neurodegenerative diseases.
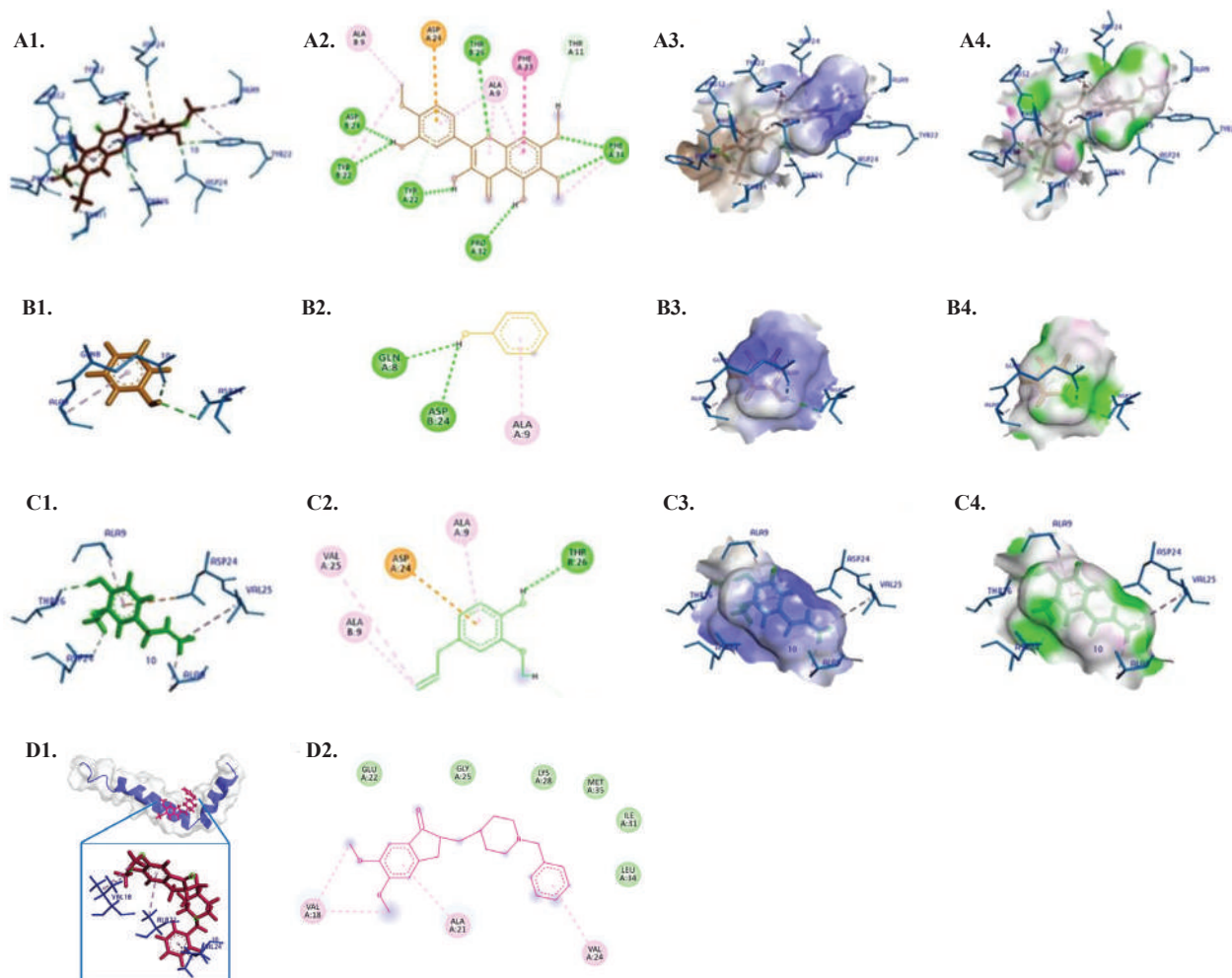
Figure 5. Two-dimensional (2D) and 3D interactions of the EEOS compounds with Aβ. A1: 3D interaction between flavonoid K (red) and Aβ active site (blue); A2: 2D hydrogen-bonding, hydrophobic, and electrostatic interactions in flavonoid K-Aβ complex; A3: 3D hydrophobic interactions in flavonoid K-Aβ complex; A4: 3D hydrogen-bonding interactions in flavonoid K-Aβ complex. B1: 3D interaction between phenol (yellow) and Aβ active site (blue); B2: 2D hydrogen-bonding and hydrophobic interactions in phenol-Aβ complex; B3: 3D hydrophobic interactions in phenol-Aβ complex; B4: 3D hydrogen-bonding interactions in phenol-Aβ complex. C1: 3D interaction between eugenol (green) and Aβ active site (blue); C2: 2D hydrogen-bonding, hydrophobic, and electrostatic interactions in eugenol-Aβ complex; C3: 3D hydrophobic interactions in eugenol-Aβ complex; C4: 3D hydrogen-bonding interactions in eugenol-Aβ complex. D1: 3D interaction between Donepezil (red) and Aβ active site (blue); D2: 2D hydrogen-bonding, hydrophobic, and van der Waals interactions in Donepezil-Aβ complex.

Acknowledgments

Authors Contribution

HW and DLK were involved in the conceptualization of the study and methodology. DRT participated in the use of *in silico* software. DAR, DA, and UK were involved in the validation process. DAR and DA conducted the formal analysis. DAR and DA conducted the investigation for the study. HW, DLK, and WW provided the resources for the study. DAR, DA, UK, and DRT were involved in the data curation. HW and UK prepared the original manuscript draft, while HW, WW, and DLK reviewed and edited the manuscript. DRT, DA and UK provided the visualization (figures and table) of the data. HW and DLK supervised the study. UK and HW took care of the project administration, whilE DLK involved in the funding acquisition All authors have read and agreed to the published version of the manuscript.

References

1. Zeng H, Sanes JR. Neuronal cell-type classification: Challenges, opportunities and the path forward. Nat Rev Neurosci. 2017; 18(9): 530-46.

2. Chi H, Chang HY, Sang TK. Neuronal cell death mechanisms in major neurodegenerative diseases. Int J Mol Sci. 2018; 19(10): 3082. doi: 10.3390/ijms19103082.

3. Dugger BN, Dickson DW. Pathology of neurodegenerative diseases. Cold Spring Harb Perspect Biol. 2017; 9(7): a028035. doi: 10.1101/cshperspect.a028035.

4. Long JM, Holtzman DM. Alzheimer disease: An update on pathobiology and treatment strategies. Cell. 2019; 179(2): 312-39.

5. Meiliana A, Dewi NM, Wijaya A. New insight in the molecular mechanisms of neurodegenerative disease. Indones Biomed J. 2018; (1): 16-34.

6. Amarya S, Singh K, Sabharwal M. Ageing process and physiological changes. In: D'Onofrio G, Greco A, Daniele Sancarlo, editors. Gerontology. London: IntechOpen; 2018. doi: 10.5772/intechopen.76249.

7. Shaw LM, Korecka M, Clark CM, Lee VM, Trojanowski JQ. Biomarkers of neurodegeneration for diagnosis and monitoring therapeutics. Nat Rev Drug Discov. 2007; 6(4): 295-303.

8. Landen JW, Cohen S, Billing CB, Cronenberger C, Styren S, Burstein AH, et al. Multiple-dose ponezumab for mild-to-moderate Alzheimer's disease: Safety and efficacy. Alzheimers Dement. 2017; 3(3): 339-47.

9. Honig LS, Vellas B, Woodward M, Boada M, Bullock R, Borrie M, et al. Trial of solanezumab for mild dementia due to Alzheimer's disease. N Engl J Med. 2018; 378(4): 321-30.

10. Nikolcheva T, Lasser R, Ostrowitzki S, Scheltens P, Boada M, Dubois B, et al. CSF and amyloid pet biomarker data from scarlet road - a global phase 3 study of gantenerumab in patients with prodromal AD. Neurobiol Aging. 2016; 39: S28-9.

11. Salloway S, Honigberg LA, Cho W, Ward M, Friesenhahn M, Brunstein F, et al. Amyloid positron emission tomography and cerebrospinal fluid results from a crenezumab anti-amyloid-beta antibody double-blind, placebo-controlled, randomized phase II study in mild-to-moderate Alzheimer's disease (BLAZE). Alzheimers Res Ther. 2018; 10(1): 96. doi: 10.1186/s13195-018-0424-5.

12. Rasool M, Malik A, Qureshi MS, Manan A, Pushparaj PN, Asif M, et al. Recent updates in the treatment of neurodegenerative disorders using natural compounds. Evid Based Complement Alternat Med. 2014; 2014: 979730. doi: 10.1155/2014/979730.

13. Mataram MBA, Hening P, Harjanti FN, Karnati S, Wasityastuti W, Nugrahaningsih DAA, et al. The neuroprotective effect of ethanolic extract Ocimum sanctum Linn. in the regulation of neuronal density in hippocampus areas as a central autobiography memory on the rat model of Alzheimer's disease. J Chem Neuroanat. 2021; 111: 101885. doi: 10.1016/j.jchemneu.2020.101885.

14. Raditya MN, Bagus AMM, Kustiati U, Wihadmadyatami H, Kusindarta DL. Data of the expression of serotonin in Alzheimer's disease (AD) rat model under treatment of ethanolic extract Ocimum sanctum Linn. Data Brief. 2020; 30: 105654. doi: 10.1016/j.dib.2020.105654.

15. Kusindarta DL, Wihadmadyatami H, Haryanto A. The analysis of hippocampus neuronal density (CA1 and CA3) after Ocimum sanctum ethanolic extract treatment on the young adulthood and middle age rat model. Vet World. 2018; 11(2): 135-40.

16. Abiola TS, David OO, Olatunde FE. Effect of tannin-rich extract of Chasmanthera dependens on piroxicam-induced liver damage in male wistar rats. Mol Cell Biomed Sci. 2021; 5(1): 27-36.

17. Pujimulyani D, Yulianto WA, Setyawati A, Rizal R, Qodariah RL, Khoiriyah Z, et al. Curcuma mangga Val. extract as antidiabetic agent in 3T3-L1 adipocyte cells. Mol Cell Biomed Sci. 2020; 4(1): 45-51.

18. Wahdaningsih S, Wahyuono S, Riyanto S, Murwanti R. Lymphocyte proliferation and nitric oxide-producing activities of lupeol isolated from red dragon fruit (Hylocereus polyrhizus) extract. Mol Cell Biomed Sci. 2021; 5(1): 8-12.

19. Sharifi-Rad M, Lankatillake C, Dias DA, Docea AO, Mahomoodally MF, Lobine D, et al. Impact of natural compounds on neurodegenerative disorders: From preclinical to pharmacotherapeutics. J Clin Med. 2020; 9(4): 1061. doi: 10.3390/jcm9041061.

20. Kusindarta DL, Wihadmadyatami H, Haryanto A. Ocimum sanctum Linn. stimulate the expression of choline acetyltransferase on the human cerebral microvascular endothelial cells. Vet World. 2016; 9(12): 1348-54.

21. Hening P, Mataram MBA, Wijayanti N, Kusindarta DL, Wihadmadyatami H. The neuroprotective effect of Ocimum sanctum Linn. ethanolic extract on human embryonic kidney-293 cells as in vitro model of neurodegenerative disease. Vet World. 2018; 11(9): 1237-43.

22. Crowley LC, Marfell BJ, Waterhouse NJ. Analyzing cell death by nuclear staining with Hoechst 33342. Cold Spring Harb Protoc. 2016; 2016(9): 778-81.

23. Santoso S, Wihadmadyatami H, Bakchoul T, Werth S, Al-Fakhri N, Bein G, et al. Antiendothelial αvβ3 antibodies are a major cause of intracranial bleeding in fetal/neonatal alloimmune thrombocytopenia. Arterioscler Thromb Vasc Biol. 2016; 36(8): 1517-24.

24. Tejera D, Mercan D, Sanchez-Caro JM, Hanan M, Greenberg D, Soreq H, et al. Systemic inflammation impairs microglial Aβ clearance through NLRP3 inflammasome. EMBO J. 2019; 38(17): e101064. doi: 10.15252/embj.2018101064.

25. Nguyen TTM, Gillet G, Popgeorgiev N. Caspases in the developing central nervous system: Apoptosis and beyond. Front Cell Dev Biol. 2021; 9: 702404. doi: 10.3389/fcell.2021.702404.

26. Kustiati U, Wihadmadyatami H, Kusindarta DL. Dataset of phytochemical and secondary metabolite profiling of holy basil leaf (Ocimum sanctum Linn) ethanolic extract using spectrophotometry, thin layer chromatography, Fourier transform infrared spectroscopy, and nuclear magnetic resonance. Data Brief. 2021; 40: 107774. doi: 10.1016/j.dib.2021.107774.

27. Harisna AH, Nurdiansyah R, Syaifie PH, Nugroho DW, Saputro KE, Firdayani, et al. In silico investigation of potential inhibitors to main protease and spike protein of SARS-CoV-2 in propolis. Biochem Biophys Rep. 2021; 26: 100969. doi: 10.1016/j.bbrep.2021.100969.

28. Nisticò R, Borg JJ. Aducanumab for Alzheimer's disease: A regulatory perspective. Pharmacol Res. 2021; 171: 105754. doi: 10.1016/j.phrs.2021.105754.

29. Marsh J, Alifragis P. Synaptic dysfunction in Alzheimer's disease: The effects of amyloid beta on synaptic vesicle dynamics as a novel target for therapeutic intervention. Neural Regen Res. 2018; 13(4): 616-23.

30. Caccamo A, Branca C, Piras IS, Ferreira E, Huentelman MJ, Liang WS, et al. Necroptosis activation in Alzheimer's disease. Nat Neurosci. 2017; 20(9): 1236-46.

31. Ayaz M, Sadiq A, Junaid M, Ullah F, Ovais M, Ullah I, *et al.* Flavonoids as prospective neuroprotectants and their therapeutic propensity in aging associated neurological disorders. Front Aging Neurosci. 2019; 11: 155. doi: 10.3389/fnagi.2019.00155.

32. Devi S, Kumar V, Singh SK, Dubey AK, Kim JJ. Flavonoids: Potential candidates for the treatment of neurodegenerative disorders. Biomedicines. 2021; 9(2): 99. doi: 10.3390/biomedicines9020099.

33. Arruda HS, Neri-Numa IA, Kido LA, Maróstica Júnior MR, Pastore GM. Recent advances and possibilities for the use of plant phenolic compounds to manage ageing-related diseases. J Funct Foods. 2020; 75(12): 104203. doi: 10.1016/j.jff.2020.104203.

34. Caruso G, Godos J, Privitera A, Lanza G, Castellano S, Chillemi A, *et al.* Phenolic acids and prevention of cognitive decline: polyphenols with a neuroprotective role in cognitive disorders and Alzheimer's disease. Nutrients. 2022; 14(4): 819. doi: 10.3390/nu14040819.